

# The Pyridine Nucleotide Cycle

STUDIES IN *ESCHERICHIA COLI* AND THE HUMAN CELL LINE D98/AH2\*

(Received for publication, September 12, 1980, and in revised form, April 8, 1981)

David Hillyard, Martin Rechsteiner, Purita Manlapaz-Ramos, Julita S. Imperial‡, Lourdes J. Cruz‡, and Baldomero M. Olivera

From the Department of Biology, University of Utah, Salt Lake City, Utah 84112 and the ‡Department of Biochemistry, University of the Philippines College of Medicine, Manila, Philippines

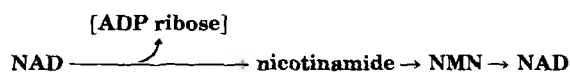
Different metabolic steps comprise the pyridine nucleotide cycles in *Escherichia coli* and in the human cell line HeLa D98/AH2. An analysis of the <sup>32</sup>P-labeling patterns *in vivo* reveals that in *E. coli*, pyrophosphate bond cleavage of intracellular NAD predominates, while in the human cell line, cleavage of the nicotinamide ribose bond predominates.

In *E. coli*, intracellular NAD is processed differently from extracellular NAD. Conversion of intracellular NAD to nicotinic acid mononucleotide (NaMN) can be demonstrated in intact cells. We have also assayed and purified an enzyme, NMN deamidase, which converts NMN to NaMN. These data suggest that in *E. coli*, the predominant intracellular pyridine nucleotide cycle operative under our experimental conditions is:



Thus, a metabolic event requiring pyrophosphate bond cleavage of NAD, such as DNA ligation, initiates most NAD turnover.

In the human cell line, the data are consistent with the following NAD turnover cycle:



Whereas in *E. coli*, ADP-ribosylation does not make a quantitatively important contribution, we suggest that in HeLa cells, ADP-ribosylation events initiate NAD turnover.

Although it has been years since Gholson (1) first proposed the continual breakdown and resynthesis of pyridine nucleotides within cells, the metabolic functions of such cycles remain undefined. To evaluate the role of a pyridine nucleotide cycle, it is desirable to determine the biochemical steps in the cycle and the magnitude at which the cycle operates *in vivo*. Previous measurements from our laboratory yielded a value for the half-life of NAD in the bacterium *Escherichia coli* of over 2 h (~140 molecules of NAD turning over/s/cell) (2); for the human cell line HeLa D98/AH2, the corresponding value was approximately 1 h (~10<sup>5</sup> molecules of NAD turning over/s/cell) (3). Thus the magnitude of NAD turnover in the

\* This work was supported by National Institutes of Health Grants GM25654 and GM24617. The work at the University of the Philippines was supported by a grant from the University of the Philippines Natural Science Research Center, an equipment grant from the Rockefeller Foundation, and the use of teaching equipment provided by the China Medical Board of New York. The costs of publication of this article were defrayed in part by the payment of page charges. This article must therefore be hereby marked "advertisement" in accordance with 18 U.S.C. Section 1734 solely to indicate this fact.

human cell line is greater than in *E. coli* (4). We also presented evidence that in *E. coli*, there are two distinguishable pyridine nucleotide cycles: a minor cycle which involves nicotinamide as an intermediate and a major cycle which does not (2).

In this study, we demonstrate that there are different breakdown pathways for intracellular and extracellular NAD in *E. coli*, and that in the intracellular cycle, cleavage across the pyrophosphate bond of NAD predominates. Also presented here are data suggesting that the metabolic steps of the pyridine nucleotide cycle in HeLa cells are quite different from the corresponding cycle in *E. coli*. Although intracellular ADP-ribosylation events (5) are negligible in rapidly growing *E. coli* cells, they may be the main biochemical event leading to NAD turnover in HeLa cells, since cleavage at the nicotinamide-ribose bond predominates.

## MATERIALS AND METHODS<sup>1,2</sup>

### RESULTS

*The Two Phosphate Groups of NAD Turn Over at Different Rates in E. coli*—To determine the intracellular pathway of NAD turnover *in vivo*, a double-label, pulse-chase experiment was performed using an exponentially growing culture of *E. coli*. The basic rationale behind this experiment is that any part of the NAD molecule which separates from the nicotinamide moiety during NAD turnover should have a low probability of returning to the NAD pool; the nicotinamide moiety and its derivative nucleoside or nucleotide, in contrast, would have a high probability of returning to the NAD pool, since in exponentially growing *E. coli*, nicotinamide has no other metabolic fate than to be ultimately converted to NAD or NADP (8).

Cells were labeled with [<sup>3</sup>H]nicotinic acid and inorganic [<sup>32</sup>P]phosphate for many generations. When the cell density reached 3 × 10<sup>8</sup> cells/ml, the cells were filtered and resuspended in unlabeled medium. NAD was purified from samples taken at various times during the chase period, and a portion of the purified NAD was cleaved with venom phosphodiesterase to AMP and NMN. Venom-treated and control samples

<sup>1</sup> Portions of this paper (including "Materials and Methods," Figs. 1-6, and Table I) are presented in miniprint as prepared by the authors. Miniprint is easily read with the aid of a standard magnifying glass. Full size photocopies are available from the Journal of Biological Chemistry, 9650 Rockville Pike, Bethesda, MD 20814. Request Document No. 80M-1929, cite author(s), and include a check or money order for \$4.80 per set of photocopies. Full size photocopies are also included in the microfilm edition of the Journal that is available from Waverly Press.

<sup>2</sup> The abbreviations used are: NaMN, nicotinic acid mononucleotide; NaAD, nicotinic acid adenine dinucleotide; ADPR, adenosine diphosphate ribose; Tris, tris(hydroxymethyl)aminomethane; Nm, nicotinamide; R, ribose.

of the purified NAD were then analyzed by paper chromatography. Typical results are shown in Fig. 1. Using such chromatographic analysis, it is possible to determine the  $^{32}\text{P}/^3\text{H}$  ratio for untreated NAD, the  $^{32}\text{P}/^3\text{H}$  ratio for NMN, and the relative amount of  $^{32}\text{P}$  in the NMN and AMP moieties of NAD. Immediately after transfer from the labeled medium, the  $[\text{}^{32}\text{P}]\text{AMP}/[\text{}^{32}\text{P}]\text{NMN}$  ratio was always between 0.90 and 1.05, showing that equilibration had been attained. The amount of  $^{32}\text{P}$  remaining in each phosphate moiety of NAD as a function of time in the chase medium was calculated from each set of chromatograms of cleaved NAD, and these results are summarized in Fig. 2. It is clear that the  $[\text{}^{32}\text{P}]\text{phosphate}$  of the AMP moiety of NAD is lost, while the  $[\text{}^{32}\text{P}]\text{phosphate}$  in the NMN moiety is largely conserved.

**NMN Produced by NAD Breakdown Can Be Deamidated to NaMN by an Enzyme in *E. coli***—The *in vivo* labeling studies above indicate that intracellular NAD breakdown involves cleavage of the pyrophosphate bond of NAD, thereby producing NMN and AMP as the initial breakdown products. During NAD turnover, the NMN phosphate group is recycled together with the pyridine ring back into the NAD pool.

While this might suggest that NMN is reincorporated into NAD without further modification, a preliminary study with crude cell extracts showed production of nicotinic acid mononucleotide from nicotinamide mononucleotide (13). We have developed an assay and purification procedure for NMN deamidase, the enzyme which catalyzes the deamidation of NMN to NaMN. As shown in Table I, the enzyme has been purified over 2,000-fold from *E. coli* extracts. By preparative gel electrophoresis, a preparation which was approximately 60% homogeneous was obtained at low yield. The enzyme showed no detectable deamidation activity toward NAD, NADP, or nicotinamide under the routine assay conditions (*i.e.* no detectable production of nicotinic acid analogues could be found after electrophoretic separation of reaction mixtures). The enzyme does not require a divalent cation (the standard assay is carried out in the presence of EDTA), and exhibits a broad peak of activity at alkaline pH values. Maximum activity was found at a pH of approximately 9; at pH 5 and lower, no activity was detected. The  $K_m$  of the enzyme for NMN under standard assay conditions is  $1.35 \times 10^{-5}$  M.

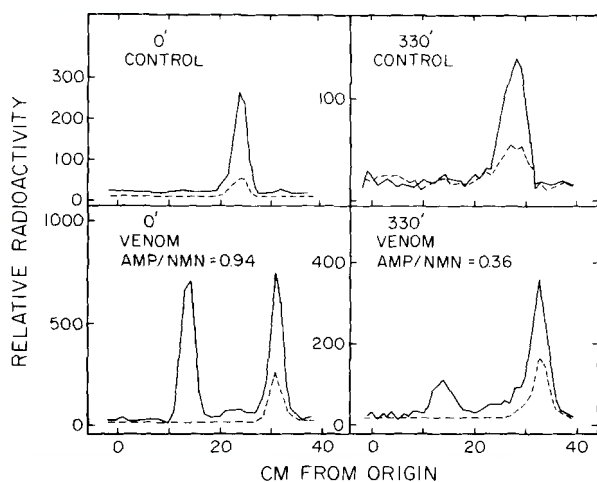


Fig. 1. Chromatographic analysis of purified NAD, and the products of venom-phosphodiesterase digestion. A culture of *Escherichia coli* H560 was labeled with  $^{32}\text{P}$  and  $^3\text{H}$ -nicotinic acid; the cells were then shifted to unlabeled medium and NAD was purified from cell culture samples at the times indicated (Methods). An aliquot of each purified NAD sample was directly analyzed by UEA paper chromatography using 0.25 M  $\text{NH}_4\text{HCO}_3$  as developing solvent; a second aliquot of each sample was treated with venom phosphodiesterase before chromatographic analysis. Analysis of samples taken at the time of the shift, and after 330 min of growth in the unlabeled medium is shown on the figure above. The dotted line represents  $^3\text{H}$  (derived from  $^3\text{H}$ -nicotinic acid) and the solid line,  $^{32}\text{P}$ . These analyses were based on complete digestion by venom phosphodiesterase. Note the change in the relative amounts of  $^{32}\text{P}$  in AMP and NMN in the zero min and 330 min sample. The peaks in the control panel ran coincident with marker NAD. After venom treatment, the slower peak is AMP, the faster, NMN.

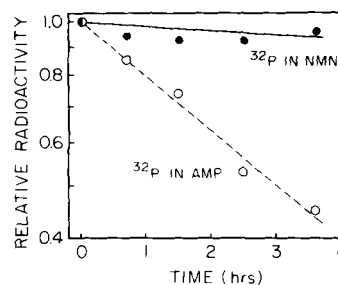


Fig. 2. The rate of loss of  $^{32}\text{P}$  from the two phosphate moieties of NAD. Relative radioactivity denotes the  $^{32}\text{P}$  normalized to the radioactivity at  $t = 0$  (time of shift to unlabeled medium). The total amount of  $^{32}\text{P}$  in NMN and in AMP was calculated for each time sample from data of the type shown in Fig. 1. For example, data at  $t = 0$ :  $^{32}\text{P}/^3\text{H}$  in NAD = 7.5;  $^{32}\text{P}/^3\text{H}$  in NMN = 3.7;  $^{32}\text{P}$  in AMP = 2248 cpm;  $^{32}\text{P}$  in NMN = 2399 cpm. Data collected at  $t = 210$  min:  $^{32}\text{P}/^3\text{H}$  in NAD = 5.3;  $^{32}\text{P}/^3\text{H}$  in NMN = 3.7;  $^{32}\text{P}$  in AMP = 1242 cpm;  $^{32}\text{P}$  in NMN = 2886 cpm. In all cases, the most variable measurement was the amount of  $^3\text{H}$  on the chromatogram (there is variable quenching of  $^3\text{H}$  on UEA paper). In order to calculate the  $^{32}\text{P}/^3\text{H}$  ratio more accurately, measurements of the  $^{32}\text{P}/^3\text{H}$  ratio for each purified NAD sample were also made using Whatman 3 MM filters, and by direct addition to scintillation fluid containing Triton X-100. The  $^{32}\text{P}/^3\text{H}$  ratio for each time point and the relative amounts of  $^{32}\text{P}$  in NMN and in AMP after venom treatment were used to calculate the amount of  $^{32}\text{P}$  in each moiety of NAD as a function of time.

Table I  
PURIFICATION OF NMN DEAMIDASE

Fraction	Total Protein mg	Total Activity units	Specific Activity units/mg	Recovery
I Extract	36,500	39,600*	1.08*	100
II Streptomycin	26,000	22,100*	0.85*	-
III Ammonium Sulfate	20,200	35,200	1.74	88.9
IV Sephadex G-75	1,200	18,000	15.0	45.5
V Hydroxyapatite	3.09	8,960	2900	22.6
VI PAGE-Fraction	-	(900)	-	(2.3)

The asterisk indicates that the assay of the crude extract and the streptomycin fraction are probably underestimates since the assays are non linear and streptomycin interferes with the assay. The figures for the polyacrylamide gel electrophoresis (PAGE) fraction are in parentheses to denote that only a portion of the hydroxyapatite fraction; fraction V was run on PAGE. The figures quoted are calculated on the basis of the whole fraction. No protein determination could be made on this fraction because of interference by gel electrophoresis reagents. However, as is described under enzyme purification, it appears that 50% of the protein in the fraction is NMN deamidase.

**Chromatography of the enzyme using Sephadex G-75** indicates an apparent native molecular weight of 33,000. Dextran blue, ovalbumin,  $\beta$ -lactoglobulin, lysozyme, and insulin were used as molecular weight standards. NMN deamidase activity was found to elute just after  $\beta$ -lactoglobulin ( $M_r = 36,800$ ). The presence of NMN deamidase suggests the following pathway for recycling the pyridine ring and phosphate group of the NMN moiety:



***E. coli* has a Different Set of NAD-breakdown Enzymes for Intracellular and Extracellular NAD**—Under the experimental conditions used above, the intracellular NAD of *E. coli* is not broken down *in vivo* to free nicotinamide or nicotinic acid to a significant extent. However, a glycohydrolase activity which does not have access to the intracellular NAD pool is present in *E. coli* cells, as shown by the experiment presented in Fig. 3. Cells grown for many generations in  $[\text{}^3\text{H}]\text{nicotinamide}$  were harvested and washed; a chromatographic analysis of intracellular radioactivity showed only NAD and NADP (Fig. 3, center panel). These cells were then incubated with exogenous double-labeled  $[\text{}^{14}\text{C}, \text{}^{32}\text{P}]\text{NAD}$  for 30 min at 37 °C. Whereas a large fraction of the intracellular NAD remained intact, the extracellular  $[\text{}^{14}\text{C}, \text{}^{32}\text{P}]\text{NAD}$  was almost completely broken down to  $[\text{}^{14}\text{C}]\text{nicotinic acid}$  (Fig. 3, top panel). The loss of radioactivity from NAD was not due to an exchange reaction, since even the  $^{32}\text{P}$  was no longer in NAD, but rather mainly  $\text{P}_i$  and possibly a minor amount of AMP. No ADPR was present. Thus, while cell extracts of *E. coli* have the ability to break down NAD to nicotinamide and nicotinic acid, in intact cells, such activities are effective only on extracellular NAD. The enzyme(s) responsible for this breakdown sediment with the cells after low speed centrifugation and must therefore be located on the cell envelope pointing outward.

Although most intracellular NAD remained intact in the

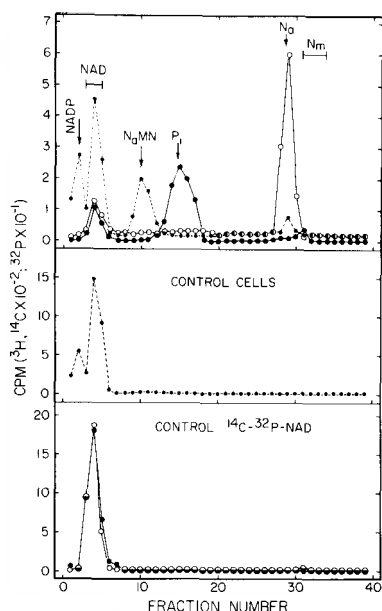


Fig. 3. Incubation of *E. coli* grown in [ $^3\text{H}$ ] nicotinamide with extracellular double-labeled [ $^{14}\text{C}$ - $^{32}\text{P}$ ]-NAD. Cells of *E. coli* strain 15T<sup>+</sup> nic<sup>+</sup>, a his<sup>-</sup> requiring strain were grown for many generations in TPG medium with [ $^3\text{H}$ ] nicotinamide. The cells were harvested and washed with unlabeled TPG. The top panel shows a chromatographic analysis of the  $^3\text{H}$ -labeled cells (ca.  $2 \times 10^8$ ) incubated for 30 min at  $37^\circ$  with extracellular [ $^{14}\text{C}$ - $^{32}\text{P}$ ]-NAD. The reaction mixture (0.05 ml) contained 95,000 cpm of [ $^{14}\text{C}$ ]-NAD, 7200 cpm of [ $^{32}\text{P}$ ]-NAD, 0.15 M sodium chloride, and 0.05 M Tris, pH 8. The reaction was stopped by adding 0.05 ml of 0.33 M HCl. Chromatography was carried out using 3 MM paper with citrate-ethanol as the developing solvent.

The small filled circles (dotted lines) are  $^3\text{H}$  radioactivity; large filled circles,  $^{32}\text{P}$ ; open circles,  $^{14}\text{C}$ .

The middle panel is a control incubation in which the  $^3\text{H}$ -labeled cells were resuspended in an identical medium, centrifuged down immediately without incubation and 0.05 ml of 0.33 N HCl added to the pellet. This allows a control analysis of the intracellular pyridine nucleotide pool when no incubation had occurred. The bottom panel shows a control incubation of [ $^{14}\text{C}$ / $^{32}\text{P}$ ]-NAD treated under identical conditions except that no *E. coli* cells were added to the incubation mixture.

It is seen from the middle panel that the  $^3\text{H}$  labeled cells originally contain only NAD and NADP (the  $^3\text{H}$ -peak traveling closest to the origin). The [ $^{14}\text{C}$ / $^{32}\text{P}$ ]-NAD, which originally travels at the NAD position (lower panel) is found mainly as [ $^{14}\text{C}$ ] nicotinic acid and inorganic phosphate- $^{32}\text{P}$  after incubation with the cells (upper panel). A new peak of  $^3\text{H}$  was also found after incubation of the cells with extracellular NAD (upper panel). This is nicotinic acid mononucleotide. These assignments were confirmed by chromatography in the DEAE- $\text{NH}_4\text{HCO}_3$  system described under Methods. The small amount of  $^3\text{H}$  nicotinic acid found after the incubation is due to a small amount of extracellular  $^3\text{H}$  label that had been incompletely removed during washing. When the cells are spun down after the incubation, the pattern was identical except for the absence of the nicotinic acid.

above incubation, some was degraded to NaMN. This indicates the intracellular location for NMN deamidase and suggests that the normal breakdown of intracellular NAD may continue even in the absence of an energy source. It is clear that *E. coli* has compartmentalized the necessary enzymatic machinery to process its intracellular NAD pool quite differently from extracellular NAD.

**Kinetics of Loss of Phosphate from the NAD Pool in Human Cells**—The turnover of NAD was examined in the human cell line D98/AH2 using the same strategy as described above for *E. coli*. In the experiment shown in Fig. 4, HeLa cells were labeled with [ $^{32}\text{P}$ ]phosphate and [ $^3\text{H}$ ]nicotinamide for 22 h. NAD was purified and cleaved with venom phosphodiesterase, and equal  $^{32}\text{P}$  radioactivity was found in the NMN and AMP phosphate moieties of NAD (Fig. 4B). After the 22-h labeling period, the cell cultures were shifted to unlabeled medium, and after growth for 8 or 16 h in unlabeled medium, analyses similar to that shown in Fig. 4 were performed. It was found that the  $^{32}\text{P}/^3\text{H}$  ratio in NAD decreased. A summary of the normalized  $^{32}\text{P}$  in the NMN and AMP moieties of NAD as a function of chase time is shown in Fig. 5. In marked contrast to the results with *E. coli* (Fig. 2), for HeLa cells, there is loss of both phosphate moieties under these growth conditions. After 16 h in chase medium, the  $^{32}\text{P}$  specific activity of the NMN moiety of NAD was less than 10% of its original value. Since the generation time of D98/AH2 HeLa cells is approximately 24 h, the observed decrease cannot be

attributed to pool expansion. Rather, the major cause of the decrease is NAD turnover.

This decrease in specific activity does not directly measure the true rate of loss of  $^{32}\text{P}$  from the NAD pool; it measures only a net loss. The net loss of radioactivity observed is the difference between the rate of loss of radioactivity from the pool and the radioactivity reentering the pool as a result of NAD resynthesis. By [ $^3\text{H}$ ]adenine labeling, the true rate of NAD breakdown ( $t_{1/2} \approx 1$  h) was previously measured (3).

From the chase experiment shown in Figs. 4 and 5, it is apparent that in HeLa cells, a significant fraction of the NAD turnover cycle involves loss of the NMN phosphate as well as the AMP phosphate. Nevertheless, these data do not allow an accurate estimate of the fraction of NAD breakdown which proceeds by this mechanism, because the half-life of NAD is short compared to the generation time of HeLa. Under such rapid turnover conditions, the problem of reincorporation of  $^{32}\text{P}$  into the NAD phosphate moieties after radioactivity has been withdrawn from the medium is significant.

Before presenting the "pool-trapping" experiments, it will be useful to consider the two most likely mechanisms of NAD turnover:

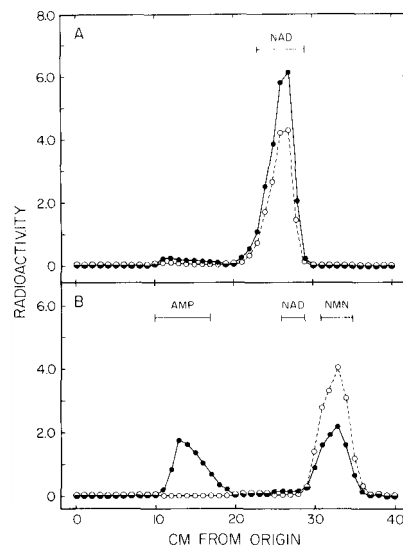


Fig. 4. Chromatographic analysis of purified and venom-treated NAD. A culture of D98/AH2 was labeled with  $^{32}\text{P}$  and  $^3\text{H}$ -nicotinamide for 22 hr. The pyridine nucleotides were extracted in acid and purified as described in Methods. One aliquot of the purified NAD sample was directly analyzed by DEAE paper chromatography; a second aliquot was treated with venom phosphodiesterase before chromatographic analysis. The solid circles represent  $^{32}\text{P}$  radioactivity (cpm  $\times 10^{-3}$ ); the open circles represent  $^3\text{H}$  radioactivity (cpm  $\times 10^{-3}$ ). Panel A is a control sample without venom treatment, and panel B is a venom phosphodiesterase treated sample. Detectable NAD is absent since it would have traveled more slowly in chromatogram A and the NaMN produced on venom treatment would have traveled more slowly than NAD in chromatogram B.

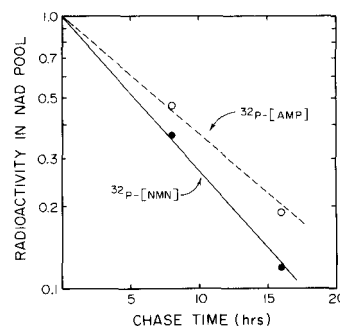
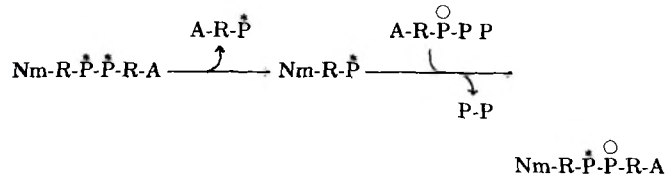
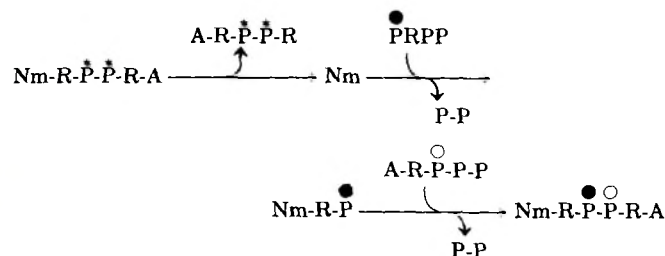


Fig. 5. Cells were labeled with [ $^3\text{H}$ ]nicotinamide and  $^{32}\text{P}$ , for 2 hr as described under Methods and then transferred into unlabeled medium for the time period indicated. The amount of  $^{32}\text{P}$  in each moiety of NAD at each time period is calculated from the values of [ $^{32}\text{P}$ -NMN]: $^3\text{H}$ -NMN and [ $^{32}\text{P}$ -AMP]: $^3\text{H}$ -NMN obtained from chromatograms similar to those shown in Fig. 4. Corrections have been made for the loss of  $^3\text{H}$  from the NAD pool ( $t_{1/2} = 8$  hr), and all values have been normalized relative to the amount of radioactivity at the beginning of the chase period.



Mechanism 1 (pyrophosphate bond cleavage)



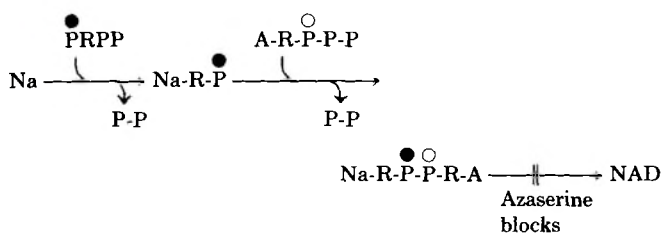
Mechanism 2 (glycosyl bond cleavage)

where Nm is nicotinamide, A is adenine, and R is ribose.

In this formulation,  $\text{Nm-R-}\overset{\bullet}{\text{P}}\text{-}\overset{\circ}{\text{P}}\text{-R-A}$  represents the specific activity of an NAD molecule at the time the radioactivity was withdrawn from the medium. The circular superscripts in  $\overset{\bullet}{\text{P}}$  and  $\overset{\circ}{\text{P}}$  represent the average specific activity of these phosphate moieties in the PRPP and ARPPP pool during the chase time. These two pathways of NAD breakdown make quite different predictions for the specific activities of the phosphate moieties in NAD at the end of a labeling/chase protocol.

To distinguish these mechanisms, it is not sufficient to measure the specific activity of the phosphate groups in NAD. It is also necessary to estimate the average specific activities

of  $\overset{\bullet}{\text{P}}$  and  $\overset{\circ}{\text{P}}$  during the chase period. Our approach has been to induce synthesis of a compound which uses the identical pools, but which is not made or accumulated under the normal growth conditions. The strategy for this pool-trapping experiment is shown below:



Unless nicotinic acid is added to the medium, no nicotinic acid adenine dinucleotide (NaAD) is synthesized, since in HeLa cells, deamidation of nicotinamide to nicotinic acid does

not occur (12). Thus, to obtain PRPP and ARPPP, nicotinic acid (Na) was added to the medium as a pulse in the middle of the period of interest. Nicotinic acid adenine dinucleotide (NaAD) was synthesized, and in the presence of azaserine, accumulated. The labeled NaAD was purified and cleaved with venom phosphodiesterase, and the products were separated by chromatography. From the specific activity of the phosphate moieties in AMP and NaMN, the average specific activity of the ARPPP and PRPP pools was calculated (an example of such a calculation is given in Footnote *a* of Table II).

Experiments which distinguish between the two alternative mechanisms of NAD turnover presented above are shown in Table II. Experiment 1 of this table is a prolonged labeling/

TABLE II

## NAD turnover mechanisms: predicted and experimental values

In Experiment 1, 75-cm<sup>2</sup> Falcon flasks were seeded with 10<sup>7</sup> D98/AH2 cells as described under "Materials and Methods." Cells were labeled for 22 h in F-12 medium containing <sup>32</sup>P, and [<sup>3</sup>H]nicotinamide (see under "Materials and Methods"), and the NAD was analyzed as described in the legend to Fig. 4. Identically labeled flasks were transferred to unlabeled medium, and after 4 h, a specific activity

determination of the precursor pools (PRPP and ARPPP) was carried out by the addition of 0.15 mg/ml of azaserine and 0.1 μg/ml of [<sup>3</sup>H]nicotinic acid (1.44 × 10<sup>5</sup> cpm/ml) (see under "Materials and Methods"). After an 8-h chase, the specific activity of the phosphate moieties of NAD was determined. From the pool-trapping experiment, the predicted values of [<sup>32</sup>P]NMN/[<sup>32</sup>P]AMP were calculated

using the experimentally determined value of  $\overset{\bullet}{\text{P}}/\overset{\circ}{\text{P}}$ . In Experiment 2, D98/AH2 cultures in 75-cm<sup>2</sup> Falcon flasks were grown in unlabeled F-12 medium and then transferred to labeled medium containing <sup>32</sup>P, and [<sup>3</sup>H]nicotinamide. The specific activity of precursor pools (PRPP and ARPPP) was determined after 2 h (see under "Materials and Methods").

The radioactivity in the phosphate moieties of NAD was determined after 4 h in the labeled medium (see Fig. 6). A label-up experiment can be analyzed exactly as the long label-chase (Experiment 1), except that the initial specific activity of the phosphate moieties of NAD ( $\text{Nm-R-}\overset{\bullet}{\text{P}}\text{-}\overset{\circ}{\text{P}}\text{-R-A}$ ) is zero (*i.e.*  $\overset{\bullet}{\text{P}} = 0$ ).

	P-R-P-P/A-R-P-P-P <sup>a</sup> (Measured in pool-trapping experiment)	[ <sup>32</sup> P]NMN/[ <sup>32</sup> P]AMP from NAD		
		Predicted value		Actual experimental value <sup>c</sup>
		Mechanism 1 <sup>b</sup>	Mechanism 2	
Experiment 1 (long label/chase)	0.54	1.53	0.54	0.78
Experiment 2 (label-up)	2.3	0.37	2.3	2.6

<sup>a</sup> PRPP and ARPPP represent the average specific activity during the chase (or labeling) period. These are experimentally measured by pool-trapping as described under "Materials and Methods." Thus, the

ratio of PRPP/ARPPP was obtained by purifying double-labeled [<sup>3</sup>H, <sup>32</sup>P]NaAD; in Experiment 1, the <sup>32</sup>P/<sup>3</sup>H ratio of the purified NaAD was 0.089. After venom phosphodiesterase treatment, [<sup>3</sup>H, <sup>32</sup>P]NaMN and [<sup>32</sup>P]AMP were produced. The actual experimental results were <sup>32</sup>P/<sup>3</sup>H in NaMN, 0.031; <sup>32</sup>P in NaMN, 148 cpm; and <sup>32</sup>P in AMP, 275 cpm. Thus [<sup>32</sup>P]NaMN/[<sup>32</sup>P]AMP can be calculated in two ways. Using only the <sup>32</sup>P, this ratio is 148/275 = 0.54. Using the <sup>32</sup>P/<sup>3</sup>H ratios, the ratio would be 0.031/(0.089 - 0.031) = 0.53. The two values, calculated independently, are in good agreement. Thus,

in Experiment 1, we have used the value PRPP/ARPPP = 0.54, since

PRPP/ARPPP = [<sup>32</sup>P]NaMN/[<sup>32</sup>P]AMP in a pulse-trapping experiment. In Experiment 2, the corresponding data are <sup>32</sup>P/<sup>3</sup>H in purified NaAD, 0.056; <sup>32</sup>P/<sup>3</sup>H in NaMN, 0.042; <sup>32</sup>P in NaMN, 57.2 cpm; and <sup>32</sup>P in AMP, 25.0 cpm. The latter values yield PRPP/ARPPP = 2.3, used in the table.

<sup>b</sup> These values are calculated correcting for the NAD synthesized *de novo* for exponential growth. It has been previously shown that 88% of the pyridine ring of NAD broken down in a D98/AH2 cell is recycled (3). Since turnover accounts for ~95% of NAD synthesis, (0.88)(0.95) or 84% of the NAD synthesized uses the recycled pyridine ring. The expected ratio of radioactivity predicted by Mechanism 1 was calculated assuming that the NMN phosphate moiety is recycled with the pyridine ring (*i.e.* at the end of the chase or labeling period,

84% of NAD will have the specific activity distribution  $\text{Nm-R-}\overset{\bullet}{\text{P}}\text{-}\overset{\circ}{\text{P}}\text{-R-A}$ , and 16% will have  $\text{Nm-R-}\overset{\circ}{\text{P}}\text{-}\overset{\circ}{\text{P}}\text{-R-A}$ . Thus, [<sup>32</sup>P]NMN/[<sup>32</sup>P]AMP

= (0.84)( $\overset{\bullet}{\text{P}}/\overset{\circ}{\text{P}}$ ) + 0.16( $\overset{\circ}{\text{P}}/\overset{\circ}{\text{P}}$ ). In the label-up experiment,  $\overset{\bullet}{\text{P}}/\overset{\circ}{\text{P}}$  = 0; in Experiment 1, the experiment value of  $\overset{\bullet}{\text{P}}/\overset{\circ}{\text{P}}$  was 1.72 as determined by pool-trapping experiments.

<sup>c</sup> These values were obtained by chromatographic analysis of pu-

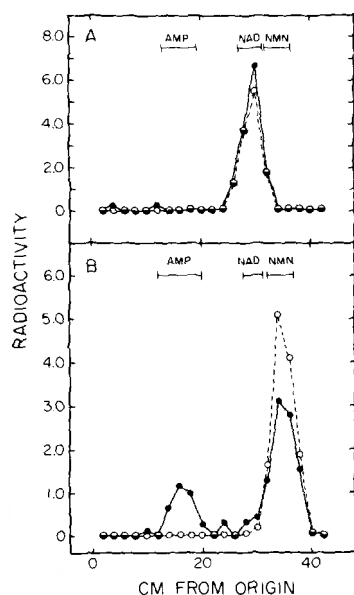


Fig. 5. Chromatography of the NAD pool extracted from cells labeled for 4 hours. A culture of D98/AH2 was labeled for a four hour period as described under Methods, and the NAD was purified. The purified NAD (panel A) and a venom phosphodiesterase treated sample (panel B) was then analyzed by chromatography on DEAE paper (see Methods). The radioactivity in 2 cm strips was then determined using a Packard Scintillation Counter, counting each sample at least twice for 10 min., and subtracting background. Radioactivity: open circles,  $^3\text{H}$ -cpm  $\times 10^{-2}$ ; closed circles,  $^{32}\text{P}$ -cpm  $\times 10^{-1}$ .

chase experiment. In addition to pool-trapping, this experiment includes the data in Fig. 5. In Experiment 2 of the table, a pulse experiment was performed (Fig. 6). Since the half-life of NAD ( $\sim 1$  h) is short compared to the generation time of HeLa ( $\sim 24$  h), most NAD synthesis ( $\sim 95\%$ ) compensates for NAD breakdown (3, 4). In addition, the pyridine ring is recycled with high efficiency (3). Therefore, it can be determined to what extent the NMN phosphate is recycled with the pyridine ring by a pulse labeling experiment (Experiment 2), using the same pool-trapping methods and analysis of the  $^{32}\text{P}$ -labeling patterns of NAD described above. Perfect recycling is represented by Mechanism 1 above; no recycling of the NMN phosphate moiety is shown by Mechanism 2.

The pool-trapping results, the expected specific activities of the phosphate groups in NAD (as predicted by the two turnover mechanisms above), and the actual specific activities obtained in each case are shown in Table II. The results clearly support Mechanism 2 (glycosyl bond cleavage) rather than Mechanism 1. Thus, when an NAD molecule breaks down within HeLa cells, both phosphate groups are lost during the turnover cycle. There is little or no recycling of the entire nicotinamide nucleotide moiety as is seen in *E. coli* cells.

#### DISCUSSION

Any metabolic event which results in the breakdown of an NAD molecule requires resynthesis of NAD to maintain intracellular levels of the coenzyme. Such a cycle of NAD breakdown and resynthesis has been referred to as the pyridine nucleotide cycle by Gholson (1). In the experiments presented above, the intracellular pyridine nucleotide cycle has been investigated in two well studied cells, *E. coli* and the human HeLa cell line D98/AH2. In both of these cells, NAD turnover is substantial, and the pyridine ring is recycled back

to the NAD pool with high efficiency ( $\sim 100\%$  in *E. coli* (8) and  $\sim 88\%$  in HeLa (3)).

The strategy of many of our experiments has been to label both the pyridine ring of NAD with  $^3\text{H}$  and the phosphate moieties with  $^{32}\text{P}$ . When radioactivity is withdrawn from the medium, it can then be determined whether  $^{32}\text{P}$  recycles with the  $^3\text{H}$ -pyridine ring back to the NAD pool after an NAD-breakdown event. There are two bonds where the initial cleavage of the NAD molecule is likely to occur: the pyrophosphate linkage, and the glycosidic bond between nicotinamide and ribose. If NAD breakdown occurs at the pyrophosphate linkage, the NMN phosphate is expected to reenter the NAD pool with the pyridine ring. However, if cleavage at the nicotinamide-ribose glycosidic bond occurs, both phosphate moieties become unlinked to the pyridine ring and therefore should have a low probability of returning to the NAD pool. We make the assumption that ADPR is not directly incorporated back into the NAD pool. That is, before the phosphate moieties in ADPR can return to NAD, they must first be converted to ATP and PRPP. This assumption is reasonable from the known biosynthetic pathways for NAD. Moreover, we have obtained direct evidence from microinjection experiments that the adenine moiety in ADPR is rapidly converted to ATP.<sup>3</sup>

Results from the double-label, pulse-chase experiments demonstrate that the major intracellular NAD turnover pathway in *E. coli* is initiated by cleavage across the pyrophosphate bond of NAD. In *E. coli* H560, the half-life of the phosphate on the AMP side is 170 min, while the rate of removal of the phosphate moiety of NMN from the NAD pool is so slow as to be barely measurable ( $t_{1/2} > 1000$  min). Thus, after an NAD-breakdown event in *E. coli*, both the pyridine ring and the NMN phosphate moiety are recycled back to the NAD pool.

In previous experiments using *E. coli* with a different genetic background (RS126), a minor pyridine nucleotide cycle with nicotinamide as an intermediate was operative at a rate of approximately 39 molecules/s/cell (2). Furthermore, cross-feeding experiments have shown that nicotinamide can be excreted by *E. coli* under certain conditions (14). In the present experiments with *E. coli* H560, we calculate that the rate of this minor pathway is less than 15 molecules/s/cell, compared to  $\sim 115$  molecules/s/cell for NMN recycling. Possibly, differences in strains or growth conditions cause some variation in the amount of breakdown to nicotinamide. In all cases we have observed, this is a minor fraction of the total intracellular pyridine nucleotide cycle in *E. coli*.

How does recycling of NMN produced by pyrophosphate cleavage of NAD take place? We have presented evidence that an enzyme is present in *E. coli* which catalyzes the deamidation of NMN to nicotinic acid mononucleotide (NaMN). NMN deamidase, which has been purified over 2000-fold, would therefore convert any NMN produced by NAD breakdown to NaMN, an intermediate in the normal biosynthetic pathway for NAD in *E. coli*. Such an activity has been reported from other bacteria (15-17). The combination of the double-label, pulse-chase experiment and the enzymological evidence that we have presented is consistent with the pyridine nucleotide cycle:



There is corollary evidence that the proposed cycle is operative under a wide variety of conditions. Our previous studies using nicotinic acid auxotrophs of *E. coli* showed that the NAD pools were gradually converted to nicotinic acid mono-

rified NAD, similar to that described in the legend to Fig. 4. The experimental data used to calculate these ratios are: Experiment 1:  $^{32}\text{P}$  in NMN, 444 cpm; and  $^{32}\text{P}$  in AMP, 570 cpm. Experiment 2:  $^{32}\text{P}$  in NMN, 845 counts; and  $^{32}\text{P}$  in AMP, 324 counts. The latter data are shown in Figure 6.

<sup>3</sup> B. Olivera, F. Haugli, and M. Capecchi, unpublished results.

nucleotide during the late starvation phase (18). If ATP became limiting in late starvation, the turnover pathway would become blocked at the step: NaMN + ATP → NaAD. These results suggest that the pyridine nucleotide cycle in *E. coli* is operative even under conditions of metabolic stress. The experiment shown in Fig. 3, in which intracellular NAD was converted to NaMN in the absence of an energy source, is consistent with this hypothesis. These data do not eliminate the possibility that at least some NMN is directly converted to NAD. However, NaAD pyrophosphorylase of *E. coli* has a much higher preference for NaMN than for NMN (19). The pathway of NAD turnover suggested above is completely consistent with DNA ligase being the initiating event, as previously suggested (2).

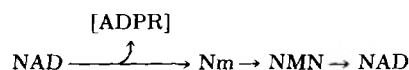
There are several possible pathways for producing nicotinamide from NAD. An NAD glycohydrolase would produce nicotinamide directly, and there is evidence that such a glycohydrolase exists in *E. coli*, since extracts can catalyze an exchange reaction between nicotinamide and NAD (20). In addition, NAD can be broken down to nicotinamide in a two-step reaction, involving the breakdown of NAD → NMN → Nm. The second enzyme in this pathway, NMN glycohydrolase, has been described for *E. coli* (21). In this study, we have not evaluated the relative contributions of these two pathways, but we have established that these activities do not affect the intracellular pool of NAD in *E. coli* under our experimental conditions. This suggests that they may be salvage enzymes which allow *E. coli* to absorb the nicotinamide ring, as well as the ribose, phosphate, and adenine moieties of any extracellular NAD. The fact that nicotinic acid auxotrophs of *Escherichia coli* can use NAD as the only source of the pyridine ring lends credence to this suggestion (22). Although *E. coli* has enzymatic activities which completely degrade NAD, these glycohydrolytic activities are apparently located in the cell envelope pointing outward, since they do not seem to be effective on the intracellular pool of *E. coli*.

Finally, the present evidence clearly eliminates ADP-ribosylation as a major contributor to NAD turnover in *E. coli* during normal exponential growth. ADP-ribosylation would lead to the loss of both phosphates of NAD during the turnover cycle, yet the NMN phosphate is recycled with high efficiency.

In contrast to *E. coli*, NAD turnover in HeLa cells does result in the loss of both phosphate groups and recycling of the nicotinamide moiety alone. As was previously shown, even the nicotinamide moiety is not completely recycled under the experimental conditions used. A certain fraction of the nicotinamide formed upon NAD breakdown (~12%) is released into the medium.

The possibility that the initial event in NAD turnover is cleavage across the pyrophosphate linkage has not been rigorously eliminated by the experiments described here. It is possible that the HeLa pyridine nucleotide cycle involves NAD → NMN → nicotinamide → NMN → NAD. Such a pathway would also result in the loss of both phosphates during NAD turnover. We believe that the possibility is unlikely, since it involves the wasteful breakdown and resynthesis of NMN. Since eukaryotic cells contain an enzyme that ADP-ribosylates nuclear proteins (5), by far the more likely possibility is that the pyridine nucleotide cycle in D98/AH2

consists of the following pathway:



The results clearly contrast those obtained in *E. coli*. In *E. coli* H560 growing under exponential conditions, an NAD molecule has less than a 50% probability of cleavage to nicotinamide and ADPR after 1000 min of growth. Intracellular ADP-ribosylation occurs at a rate of less than 15 molecules/s/cell. In contrast, in HeLa D98/AH2 cells, most, and possibly all NAD turnover events involve the loss of both phosphate moieties, consistent with ADP-ribosylation being the main pathway for NAD turnover.

The data above clearly indicate that the metabolic steps in the pyridine nucleotide cycle of the prokaryotic *E. coli* and eukaryotic HeLa cells are different. Such differences may well reflect differences in the function of prokaryotic and eukaryotic pyridine nucleotide cycles. DNA ligation and protein ADP-ribosylation may be the major underlying reasons for prokaryotic and eukaryotic pyridine nucleotide cycles, respectively.

#### REFERENCES

- Gholson, R. K. (1966) *Nature (Lond.)* **212**, 933
- Manlapaz-Fernandez, P., and Olivera, B. M. (1973) *J. Biol. Chem.* **248**, 5150-5155
- Rechsteiner, M., Hillyard, D., and Olivera, B. M. (1976) *J. Cell. Physiol.* **88**, 207-217
- Rechsteiner, M., Hillyard, D., and Olivera, B. M. (1976) *Nature* **259**, 695-696
- Hayaishi, O., and Ueda, K. (1977) *Annu. Rev. Biochem.* **46**, 95-116
- Laskowski, M., Jr. (1966) in *Procedures in Nucleic Acid Research* (Cantoni, G. L., and Davies, D. R., eds) p. 168, Harper & Row, New York
- Dürwald, H., and Hoffmann-Berling, H. (1971) *J. Mol. Biol.* **58**, 755-773
- Lundquist, R., and Olivera, B. M. (1971) *J. Biol. Chem.* **246**, 1107-1116
- Sinsheimer, R. L. (1966) in *Procedures in Nucleic Acid Research* (Cantoni, G. L., and Davies, D. R., eds) pp. 569-576, Harper & Row, New York
- Witholt, B. (1971) *Methods Enzymol.* **18**, 813-816
- Ham, R. G. (1965) *Proc. Natl. Acad. Sci. U. S. A.* **53**, 288-293
- Hillyard, D., Rechsteiner, M. C., and Olivera, B. M. (1973) *J. Cell. Physiol.* **82**, 165-180
- Cruz, L. J., Salabao, J. L., Flores, E., and Olivera, B. M. (1974) *Technical Report No. 18*, pp. 1-25, University of the Philippines Natural Science Research Center, Diliman, Quezon City, Philippines
- Andreoli, A. J., Grover, T., Gholson, R. K., and Matney, T. S. (1969) *Biochim. Biophys. Acta* **192**, 539-541
- Friedmann, H. C. (1971) *Methods Enzymol.* **18B**, 192-197
- Friedmann, H. C., and Gartski, C. (1973) *Biochem. Biophys. Res. Commun.* **50**, 54-58
- Kinney, D. M., Foster, J. W., and Moat, A. G. (1979) *J. Bacteriol.* **140**, 607-611
- Lundquist, R., and Olivera, B. M. (1973) *J. Biol. Chem.* **248**, 5137-5143
- Dahmen, W., Webb, B., and Preiss, J. (1967) *Arch. Biochem. Biophys.* **120**, 440-450
- McLaren, J. (1973) Ph.D. thesis, Kansas State University, Manhattan, Kans.
- Andreoli, A. J., Okita, T. W., Bloom, R., and Grover, T. A. (1972) *Biochem. Biophys. Res. Commun.* **49**, 264-269
- Gholson, R. K., Tritz, G. J., Matney, T. S., and Andreoli, A. J. (1969) *J. Bacteriol.* **99**, 895-896

SUPPLEMENTAL MATERIAL TO  
THE PYRIDINE NUCLEOTIDE CYCLE. STUDIES IN *ESCHERICHIA COLI*  
AND THE HUMAN CELL LINE D98/AH2

David Hilliard, Martin Rechsteiner, Purita M. Ramos, Jullita S. Inderial,  
Lourdes J. Cruz and Baldobero M. Yllaveza

MATERIALS AND METHODS

**Materials:** [<sup>3</sup>H]-nicotinamide (3 × 10<sup>5</sup> cpm/μg), [<sup>3</sup>H]-nicotinic acid (1.14 × 10<sup>6</sup> cpm/μg) and [<sup>14</sup>C]-nicotinamide-NAD (53 Ci/mole) were purchased from Amersham Searle, [<sup>32</sup>P]-NAD (22 mCi/μmole) and [<sup>32</sup>P] (carrier free) were purchased from New England Nuclear Corporation. Millipore filters were obtained from Schleicher and Schuell, Penassay Broth from Difco Corporation, nicotinic acid and azaserine from Calbiochemical Co., and DEAE paper from W. Reeve Angel Company. Unless otherwise specified, all other biochemicals were obtained from Sigma. Venom phosphodiesterase from Sigma was further purified using a Dowex 50 column (b). Bacterial strains--For these experiments, *E. coli* H560, a pol<sup>+</sup> endo<sup>+</sup> thy<sup>+</sup> strain (?) and *E. coli* 151<sup>+</sup> nic<sup>+</sup> (8) were used.

**Growth of Bacterial Cells:** *Escherichia coli* H560 was grown at 37°C in 30 ml of a defined low phosphate tris-phosphate-glucose medium (TPG) (9) supplemented with 4 μg per ml of thymine, 3 μg per ml of [<sup>3</sup>H]-nicotinic acid (1.14 × 10<sup>6</sup> cpm/μg) and 2.5 mCi of [<sup>32</sup>P] (carrier-free) for many generations. When the cell density was about 3 × 10<sup>8</sup> cells per ml, 20 ml of the culture was filtered on a Millipore filter (0.45 μ pore size, boiled for 10 minutes), washed with 10 μ containing 2 μg/ml of unlabeled nicotinic acid and 4 μg/ml of thymine, and then resuspended in 100 ml of Penassay Broth containing 2 μg/ml of nicotinic acid. Cell density was followed using a Coulter counter and intracellular radioactivity was determined by filtering 10 μ of culture on the Millipore filter, washing with Penassay Broth and counting the dried filter in a liquid scintillation counter at various times before and after the shift to unlabeled medium. After the culture was shifted to unlabeled medium, cells were grown at 37°C and 5 ml samples were taken at various times for the isolation of NAD. During the prolonged chase period the medium was diluted so that the cells remained in exponential growth phase and never exceeded 5 × 10<sup>8</sup> cells per ml.

**Isolation of NAD from Bacterial Cells:** The culture samples were centrifuged for 10 minutes at 7,000 rpm in a Sorvall RC-28 Centrifuge and the supernatant discarded. The cells were suspended in 0.25 ml of 0.33 M HCl, and sonically irradiated using a Branson sonifier microtip (3x, 0.5 minutes). An aliquot (2 μl) of the extract was counted on a liquid scintillation counter before and after centrifugation in an Eppendorf centrifuge for 1 minute.

After centrifugation the supernatant (0.2 ml) was neutralized using 1 M NaOH, diluted at least 20-fold, loaded on a DEAE Sephadex column (0.5 cm diameter, 5 cm height, A-25-120 DEAE Sephadex), washed with 2 ml of 0.005 M Tris, pH 7.6 and the NAD was finally eluted using 0.05 M Tris, pH 7.6.

The NAD fractions were pooled and reduced to NADH using alcohol dehydrogenase. For each ml of the pooled fractions of NAD were added 0.05 ml of 4 M ethanol, 5 μl of 0.05 M magnesium chloride, 3 μl of 40 mg/ml NAD and 10 μl of alcohol dehydrogenase (1 mg/ml). The increased absorbance at 340 nm of the mixture after enzyme addition was compared to that of a control using 0.05 M Tris, pH 7.6, and complete reduction of NAD was reached after 10 minutes at 37°C.

The reduced NAD was loaded on a second DEAE Sephadex column equilibrated with 0.07 M Tris, pH 7.6, and the column was washed with this buffer until no further [<sup>32</sup>P] counts were eluted. The NADH was then eluted using 0.5 M Tris, pH 7.6. The peak NADH fraction was reoxidized by adding to each ml of the peak NADH fraction: 0.02 ml of 2 M sodium pyruvate, 10 μl of 0.05 M magnesium chloride and 10 μl of lactate dehydrogenase (20 mg/ml; 80 units per mg protein). The mixture was incubated for 15 min at 37°C, and oxidation was monitored by decreased absorbance at 340 nm.

An aliquot of the purified NAD was cleaved with venom phosphodiesterase by adding 5 μl of venom phosphodiesterase (1 mg/ml) to 0.1 ml of the purified NAD sample. After enzyme digestion for 20 min at 37°C, both treated and untreated NAD samples were analyzed using paper chromatography.

**Chromatography:** Chromatography was performed either on DEAE paper (Whatman DE 81) using 0.25 M ammonium bicarbonate as solvent or on 3 MM paper (Whatman) in solvent containing one part 96.3 g ammonium chloride, 6.24 g citric acid and 23.04 g sodium citrate in 900 ml of distilled water and 3 parts of 95% ethanol (10). Chromatography using the citrate-ethanol system was generally for 24-36 hr. After development, 1 cm strips were analyzed for 3H, <sup>14</sup>C and <sup>32</sup>P radioactivity using a Beckmann liquid scintillation counter.

**Culture and Labeling of HeLa Cells:** The heteroploid human cell line, D98/AH2, was obtained from the American Type Culture Collection (Cell 183) and routinely cultured in F12 medium (11) containing 5% fetal calf serum. The medium and all other tissue culture solutions was heated at 56°C for 30 min prior to their use, and periodic tests for mycoplasma contamination were consistently negative.

Before labeling, 75 cm<sup>2</sup> plastic T-flasks containing approximately 10<sup>7</sup> cells were rinsed twice with F12 medium lacking niacin, tryptophan and phosphate. The labeling medium contained [<sup>32</sup>P] (10 μCi/ml; 26.8 mg/l, ten times lower than normal), [<sup>3</sup>H]-nicotinamide (1 μg/ml; 3 × 10<sup>5</sup> cpm/μg) and 5% dialyzed fetal calf serum. The cells were transferred from labeling medium by twice rinsing each flask with complete F12 medium and growth was continued at 37°C in complete F12 medium.

For the "pool-trapping" of NaAD (see Results), 0.15 mg/ml azaserine and 0.1 μg/ml [<sup>3</sup>H]-nicotinic acid (specific activity 1.44 × 10<sup>6</sup> cpm/μg) were added to F12 medium. Cells were grown in this medium for 1.5 hr at 37°C, washed, and the pyridine nucleotides extracted by adding 0.5 to 1.0 ml of 0.03 M HCl as previously described (12). NaAD was purified and analyzed as described below.

**Purification of NAD and NaAD from HeLa Cells:** NAD was purified as described above for bacterial cells. To purify NaAD, the 0.03 M HCl extracts were titrated to pH 7.0 with 1 M sodium hydroxide and then loaded onto a DEAE Sephadex A25-120 column (0.4 × 4 cm) equilibrated with 5 mM Tris pH 7.6. The column was washed successively with 3 ml portions of 0.005 M, 0.05 M, 0.075 M, 0.1 M and 0.2 M of Tris, pH 7.6, and 0.5 ml fractions were collected. NaAD eluted at 0.1 M Tris, pH 7.6; fractions containing 3H which eluted at this salt concentration were spotted on 3 MM paper (approximately 3 cm<sup>2</sup> ml of sample). After chromatography for 24 hr, the NaAD peak was located by cutting 1 cm wide strips from both edges of the spotting area; these chromatogram strips were counted to locate NaAD, and the region of the middle strip containing most of the labeled NaAD was cut out. NaAD was eluted using distilled water. The purified NaAD chromatographed with authentic NaAD on both the 3 MM paper, citrate-ethanol system and the DEAE-paper, 0.25 M NH<sub>4</sub>HCO<sub>3</sub> solvent system. In addition, treatment of the purified NaAD with venom phosphodiesterase, yielded products which chromatographed with authentic NaMN and AMP on both chromatographic systems.

Paper chromatography was performed on venom phosphodiesterase-treated and intact NaAD. The venom phosphodiesterase digestion was carried out by adding 0.05 ml of purified NaAD to 0.2 ml of 0.1 M Tris, pH 7.6, 0.04 ml of 0.05 M magnesium chloride, 0.007 ml of 1 M sodium hydroxide, and 0.002 ml of venom phosphodiesterase (approximately 2 μg/ml). The samples were incubated at 37°C for 20 minutes, and spotted on 3 MM paper with AMP, NMN and NAD as markers. After chromatography the radioactivity was analyzed as described previously (12).

**Gel Electrophoresis:** Isoelectric focusing was done using Medical Research Apparatus (MRA) Corporation apparatus M137-IP for preparative gels and M137-A for analytical gels. Protein samples in a solution of 10% glycerol - 1% ampholyte (LKB Ampholine, pH 3.5-10) containing a few μl of 0.5% bromophenol blue as marker were applied on cylindrical polyacrylamide gels (0.3 × 10 cm for analytical and 1.3 × 2 × 10 cm for preparative scale) prepared from a solution consisting of 7.5% acrylamide, 2% bisacrylamide, 2.0% ampholyte, 5% glycerol and 0.4 mg % riboflavin. The samples were overlaid with 5% glycerol - 0.5% ampholyte and isoelectric focusing was carried out with 0.08 M NaOH as catholyte and 0.04 M H<sub>2</sub>SO<sub>4</sub> as anolyte at 200 volts for the first 2 hr and 400 volts until completed.

Polyacrylamide disc gel electrophoresis was performed in a Canalco Chamber Model 1200 or in the water cooled isoelectric focusing apparatus (MRA) when ever enzyme activity was to be recovered. Running gels were 7% acrylamide and buffered with 0.38 M Tris, pH 8.9; buffer reservoirs contained 0.02 M glycine - Tris buffer, pH 9.5. Analytical runs were done on 0.5 × 10 cm or 0.3 × 10.5 cm gels at 0.25 mA/gel for 2 hr or 0.5 mA/gel for 4-5 hr respectively. Preparative electrophoresis was carried out at a constant current of 3 and 5 mA per gel using 1.3 × 16.0 cm or 1.9 × 16.0 cm cylindrical gels. Gels were stained with Coomassie blue.

**Assay for NMN Deamidase Activity:** The reaction mixture (in a final volume of 0.020 ml) contained: 5 μmoles Tris, pH 8, 1 μmole EDTA, 50 μmole [<sup>14</sup>C]-NMN or [<sup>3</sup>H]-NMN (5000 cpm) and enzyme. The mixture was incubated for 30 min at 37°C and quenched by boiling for 3 minutes. A 0.010 ml aliquot of the incubation mixture was applied on Whatman #1 chromatography paper strips or Beckman strip #31932B with unlabeled NMN and NaMN as markers.

Paper electrophoresis was performed for 2 hr at 10 mA using a Bjerrum type paper electrophoresis setup (Beckmann) containing 0.2 M citrate buffer, pH 3.5 or pH 5.5. The strips were dried at 100°C for 15-30 minutes, cut into 0.7 cm segments and counted using a toluene based scintillation fluid. The percentage conversion was calculated from the radioactivity in the NMN and NaMN peaks.

**Purification of NMN Deamidase:** Fraction I. Cell Extract--*Escherichia coli* BB was suspended in 0.1 M Tris pH 7.2, 1 mM EDTA, 1 mM β-mercaptoethanol ("Buffer A") at a concentration of 0.75 g/ml. The cells were disrupted by sonic irradiation (Branson sonifier) in 45 ml portions, and then centrifuged at 12,000 x g for 20 min. The cell extract was diluted with more buffer to a protein concentration of 20 mg/ml (Fraction I).

**Fraction II. Streptomycin Sulfate Precipitation--**A freshly prepared 5% streptomycin sulfate solution was added to fraction I (0.2 ml/ml) and after 20 min at 0°, the solution was centrifuged. The supernatant was collected and further diluted with 5% streptomycin sulfate (0.33 ml/ml of diluted supernatant). After an additional 20 min at 0°, the solution was centrifuged, the precipitate discarded and the supernatant fluid (Fraction II) was immediately subjected to ammonium sulfate precipitation.

**Fraction III. Ammonium Sulfate Precipitation--**Ammonium sulfate (0.525 g/ml of fraction II) was added with stirring. After 30 min at 0°, the precipitate was collected by centrifugation and dissolved in a minimal volume of a 1:1 mixture of glycerol and Buffer A. This preparation can be stored for several months at -5°C without significant loss of activity (Fraction III).

**Fraction IV. Sephadex G75 Chromatography--**This step was carried out in batches of 1.1 g protein. Each batch was dialyzed (2 × 2 hours) against Buffer A to remove the glycerol and ammonium sulfate. The dialyzed fraction was concentrated by dehydration with polyethylene glycol to 1/5 of the original volume. This was applied on a Sephadex G75 column (55 × 4.5 cm) previously equilibrated with Buffer A and 10 ml fractions were collected. Fractions containing enzyme were concentrated by dehydration with solid polyethylene glycol, and diluted with an equal volume of glycerol. All fractions with a specific activity greater than 10 units/mg were combined (Fraction IV).

**Fraction V. Hydroxyapatite Chromatography--**Fraction IV (in 0.5 g batches) was dialyzed in 0.01 M potassium phosphate buffer, pH 6.8, 1 mM EDTA, 1 mM β-mercaptoethanol (Buffer B). The dialyzed fraction was concentrated with solid polyethylene glycol to 1/5 its volume, and applied to a hydroxyapatite column (40 × 4.5 cm) previously equilibrated with Buffer B. The column was eluted with Buffer B; the enzyme passes through the hydroxyapatite column. The active fractions were concentrated using polyethylene glycol, and an equivalent volume of glycerol was added. Fractions with specific activities greater than 1000 units/mg were combined (Fraction V).

**Further Purification of the Enzyme--**Additional purification steps were attempted to bring the enzyme close to homogeneity; however, the final purification steps involved gel electrophoresis which gave very poor recovery. Thus, although we have studied some properties of the enzyme using the nearly homogeneous enzyme, these steps cannot be recommended for routine purification procedures because of poor recovery. For most purposes, the hydroxyapatite fraction provides an enzyme preparation that is satisfactory (as a reagent for the conversion of NMN to NaMN, for example).

A nearly homogeneous preparation of enzyme (Fraction VI) was obtained by running a portion of Fraction V (1 mg) on 1.9 × 16 cm isoelectric focusing gels. After focusing, the gel was extruded and cut manually into 2 mm segments, which were macerated using a fine glass rod, and suspended in 0.05 M Tris buffer, pH 8, 1 mM EDTA, 1 mM β-mercaptoethanol. The fractions containing enzyme activity were pooled, sonically irradiated and after centrifugation the gel was resuspended in 0.05 M Tris buffer, pH 8, 1 mM EDTA, 1 mM β-mercaptoethanol, sonically irradiated again and centrifuged. The combined supernatants were subjected to preparative gel electrophoresis in gel tubes (1.9 × 16 cm) at a constant current of 5 mA per gel. Two mm lengths were cut and after maceration and suspension in Tris buffer, NMN deamidase was obtained in the supernatants. The amount of protein could not be assayed accurately because of the minute amounts of protein and interference from reagents in the polyacrylamide gel. However, analysis of the material obtained after preparative electrophoresis on analytical gels showed a major band containing roughly 60% of the protein (as judged by the intensity of staining) and two minor bands. This was confirmed by analytical isoelectric focusing. The enzyme activity could be recovered from the analytical gels, and the enzyme activity coincided with the major protein peak. The position of the major peak and the enzyme activity indicate that under the conditions of isoelectric focusing, the pI of NMN deamidase is 5.3.